

Oil spill fluorosensing lidar for inclined onshore or shipboard operation

Renata Karpicz, Andrej Dementjev, Zenonas Kuprionis, Saulius Pakalnis, Rainer Westphal, Rainer Reuter, and Vidmantas Gulbinas

An oil spill detection fluorosensing lidar for onshore or shipboard operation is described. Some difficulties for its operation arise from the inclined path of rays. This is due to the increased reflection of the laser beam at the air–water interface, the decreased fluorescence signal, and the increased background light when compared with other instruments having a close-to-nadir measuring geometry. The analysis of these problems shows that they significantly reduce the detection distance in the presence of a flat water surface. However, waves on the water surface weaken the influence of the laser beam reflections but at the same time cause a variable fluorescence signal, which makes specific signal processing necessary for increased detection ranges. A fluorescence data processing method is proposed that efficiently eliminates the background water column fluorescence from signals such as yellow substance. This enables oil fluorescence to be distinguished from variable natural water fluorescence. © 2006 Optical Society of America

OCIS codes: 280.3640, 300.6280, 010.3640, 120.0280.

1. Introduction

Rapid and reliable oil spill detection is an essential yet often overlooked part of oil pollution prevention and response strategies. Early warning in case of a pollution event is important to minimize its environmental and financial impact. Depending on the specific spill scenario, a delayed response may result in a larger spill volume, is likely to impact a larger total area, and will almost certainly result in a costlier cleanup effort.

There are a number of technologies that can be used for remote oil spill detection. Oil interacts with electromagnetic waves in different ways at different wavelengths. This makes it possible to use different kinds of sensor, which have their advantages and disadvantages, such as radar and microwave radiometers,¹ and multispectral imagers in the UV,² visible,³ or IR⁴ spectral range. In this field of sensors, the laser fluorosensor has the unique capability to identify oil on backgrounds that include water, beaches, soil, ice, and snow.⁵ If oils are irradiated by UV radiation, the

light is absorbed and a portion of its energy is emitted as fluorescence at longer wavelengths. Different oils yield different fluorescence spectra, and, therefore, it is possible to discriminate between certain classes of oil.⁶

In recent years, the development of laser fluorosensors has focused on improving the ability to survey large areas by using aircraft. These instruments are large and expensive, and they require highly qualified personnel and sophisticated maintenance. These limitations make their use practical only as a component of surveillance aircraft, and they have recently been used operationally by only a few agencies.^{5,7,8} While aircraft deployment has its advantages, there is also a need to monitor specific areas, such as approaches to oil trade facilities or selected parts of waterways. The area monitored in these cases might be rather limited, but it is important to ensure continuous day-and-night surveillance. Under such conditions, fluorosensors applied from small boats or mounted at fixed positions may have an advantage because of much lower costs for operation and maintenance.

The technical requirements, particularly safety regulations for this kind of fluorosensor, are not so strict. Its sensing distance may be smaller and the sampling rate for stationary devices may be much lower. However, new problems arise if instruments are mounted a few meters above the sea surface. To achieve reasonable sampling distances, scans are performed with small sampling angles between the

R. Karpicz, A. Dementjev, and V. Gulbinas (vidgulb@ktl.mii.lt) are with the Institute of Physics, Savanoriu 231, LT-02300 Vilnius, Lithuania. Z. Kuprionis and S. Pakalnis are with E Kspla UAB, Savanoriu 231, LT-02300 Vilnius, Lithuania. R. Westphal and R. Reuter are with the Institute of Physics, Carl von Ossietzky University of Oldenburg, D-26111 Oldenburg, Germany.

Received 6 February 2006; revised 7 April 2006; accepted 13 April 2006; posted 13 April 2006 (Doc. ID 67837).

0003-6935/06/256620-06\$15.00/0

© 2006 Optical Society of America

water surface and the optical axes of the laser beam and telescope.

Another problem is related to the fluorescence of natural waters. The abundance of yellow substances, which consist of a broad spectrum of light-absorbing organic macromolecules and of phytoplankton with its fluorescent pigments, causes a problem while discriminating between oil and water fluorescence. A stationary or ship-based fluorosensor is intended to operate in near-shore regions such as harbors and oil terminals, where the water contains mostly large amounts of fluorescent substances. Then the discrimination problem becomes more difficult in comparison to the problems of airborne instruments that are applied over offshore waters.

We discuss the inclined sampling problem, the design and operation of a laser fluorosensing lidar for near-shore or shipboard operation with inclined ray path is presented, and we demonstrate a simple way to discriminate between oil and water fluorescence.

2. Specific Features of Inclined Sampling

Figure 1 depicts the operation geometry of an inclined sampling lidar. The laser emits an UV light pulse toward the water surface, and the detector directed to the same water spot detects fluorescence. The laser beam directed to the water surface or oil film at a small grazing angle is partially reflected. Before reaching the receiver, the fluorescence also passes the surface at the same angle, and it is also partially reflected into the oil layer or water column. In addition to oil fluorescence, the receiver also collects the following components: water column fluorescence, elastic and Raman backscattered radiation of the laser beam, and reflected daylight.

Here we consider the intensities of the different light components in dependence on the angle between the laser beam and the normal to the water or oil surface (incidence angle α). By increasing the sampling angle, the intensity of the oil and water fluorescence collected by the detector decreases because of two factors: (a) more laser light is reflected, therefore, lower intensity penetrates into the water (or oil) and hence the laser beam initiates less fluorescence; and (b) the partial reflection of fluorescence from oil or other fluorescent substances propagating toward the detector increases. The reflection coefficients for *P*-polarized and *S*-polarized light depend on incidence angle α according to the Fresnel relations:

$$R^P = \left(\frac{n \cos \alpha - \cos \beta}{n \cos \alpha + \cos \beta} \right)^2,$$

$$R^S = \left(\frac{\cos \alpha - n \cos \beta}{\cos \alpha + n \cos \beta} \right)^2, \quad (1)$$

where n is the refractive index. The angle of refraction β is equal to

$$\beta = \arcsin\left(\frac{\sin \alpha}{n}\right). \quad (2)$$

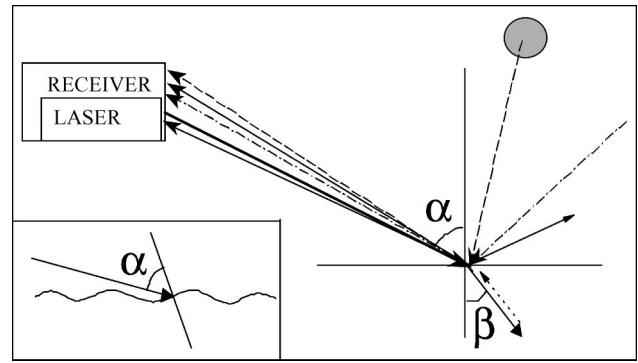


Fig. 1. Inclined fluorosensor operation geometry. The bold solid line shows the laser beam; the thin lines show various detected light components: fluorescence (solid line), scattered sunlight (dashed line), reflected skylight (dashed dotted line), and Raman-scattered laser radiation (dotted line). Inset shows the sampling geometry in case of a wavy water surface.

It is supposed that the refractive index difference at the laser wavelength and the fluorescence wavelengths is negligible, and hence, the reflection coefficient of the fluorescence light is the same as for the laser beam. Therefore fluorescence collected by the telescope passes the same trajectory as the laser beam, and the fluorescence intensity follows a $[1 - R^{P,S}(\alpha)]^2$ angular dependence. Elastic and Raman scattered light intensities follow the same dependences.

The reflected skylight intensity is proportional to $R^{P,S}$. The scattered sunlight intensity depends on the Sun orientation relative to the sampling direction. However, for waters that are not extremely turbid the scattered sunlight intensity is much weaker than the reflected skylight, if direct sun glitter is excluded. Therefore the scattered sunlight will not be further considered.

Figure 2 shows the dependences of the fluorescence and scattered skylight intensities on the sampling distance normalized to the fluorosensor height above the water surface. As can be seen, *P*-polarized excitation and detection light is advantageous because of stronger fluorescence and weaker reflected skylight. Therefore we will consider only the *P*-polarized excitation and detection geometry in the following sections. By increasing sampling distance r (the hypotenuse of the respective triangle; see Fig. 1) at a constant fluorosensor height above the water surface the detected fluorescence signal decreases as $I \propto r^{-2}[1 - R^P - (\alpha)]^2$. This dependence is much stronger than the $I \propto r^{-2}$ dependence for vertical sampling. For example, at a distance-to-height ratio equal to 10 the fluorescence intensity due to the angular factor drops down about three times in comparison with the vertical sampling, whereas the reflected skylight intensity increases by a factor of 10.

The presented dependences are valid in the case of an ideal, perfectly flat water surface. An analysis of the angular dependences shows that waves changing the sampling angle are not very important in the case of

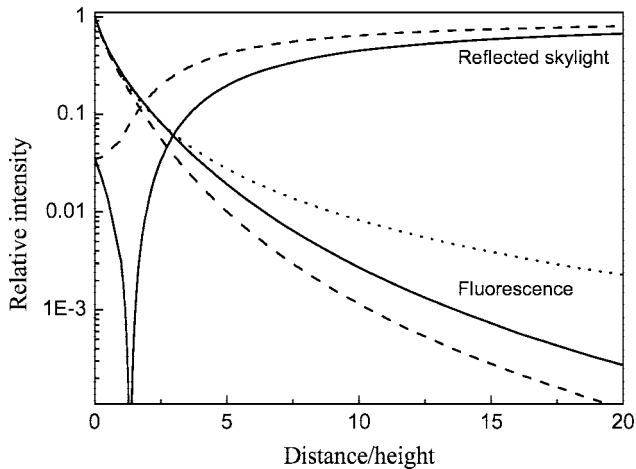


Fig. 2. Calculated fluorescence and reflected skylight intensity dependences on the sampling distance, which is normalized to the sampling height. The fluorescence intensity is normalized to its intensity at vertical sampling, while the reflected skylight intensity is normalized to its total reflection (close to horizontal sampling). Solid curves correspond to P polarized light and dashed curves to S polarizations. Dotted curve shows the fluorescence intensity dependence on the distance for vertical sampling geometry.

near-nadir sampling but have a strong influence at large sampling angles. The Fig. 1 inset shows the sampling geometry in the case of a wavy water surface. A simple estimation shows that the average reflection of a wide beam (much wider than the wave height) almost saturates when the distance-to-height ratio comes close to the ratio of half of the wavelength to the wave height. (Even from ordinary experience one knows that a wavy sea is darker since there is less skylight reflection and its color does not change starting from some particular distance). Burikov *et al.*⁹ investigated the wave influence on the fluorescence signal in the case of inclined sampling. According to their results the average fluorescence signal approaches the $I \propto r^{-2}$ dependence when the waves are sufficiently strong. Thus the sampling distance may be significantly increased due to waves. On the other hand, the waves cause variations in the sampling angle and therefore induce strong variability of the detected signal.

3. Laser Fluorosensor Description

The block scheme of the fluorosensor used in the current investigation is shown in Fig. 3. It consists of a laser with beam formation and direction optics, scanner, telescope, spectrograph, registration electronics, and a computer. The third harmonics (355 nm) of a diode pumped Q -switched Nd:YAG laser operating at a 200 Hz repetition rate is used. The laser pulse length is approximately 10 ns, and the pulse energy is 0.5 mJ. The signal collected with a 20 cm aperture diameter $f/10$ Cassegrain telescope (Model Mead 8) is directed to a polychromator. A diffraction grating splits the collected light into six detection channels with the following bandwidths: 366–395 nm, 395–433 nm, 443–480 nm, 490–555 nm, 570–636 nm,

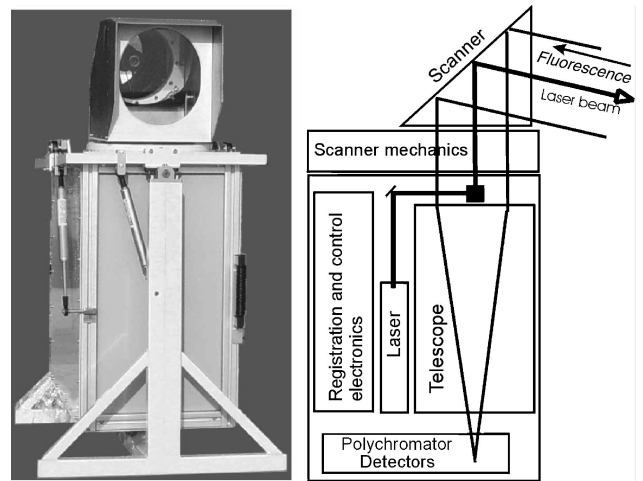


Fig. 3. Front view and schematic optomechanical layout of the laser fluorosensor.

and 640–740 nm. A 2400 line/mm grating is used and enables ± 3 nm spectral resolution. A rejecting mirror for 355 nm is situated before the grating to reject relatively strong backscattered laser light. The light in the first four channels (UV/blue/green light) is detected by compact Hamamatsu photomultipliers, Model R7400U/R7400-03U, and in the last two channels (red light) by Hamamatsu R7400-01U. A periscope-type scanner enables us to vary the sampling direction. The laser beam and the light collection direction are changed by the same mirror ensuring their unchanged overlap during the scanning process. In the fast scanning mode it scans a 120° sector with a 1 Hz repetition rate. The data collection system enables signal detection from every individual laser pulse. Thus at a 50 m sensing distance the fluorosensor probes the water surface at approximately every 1 m.

Several technical solutions enable us to reduce the influence of daylight on the detected signals. The viewing angle of the telescope only slightly exceeds the laser beam divergence. The beam diameter at a 50 m distance is approximately 10 cm and the telescope field of view is less than 20 cm. To protect the photomultipliers from nonlinear response due to signal saturation, the high voltage is applied by 4 μ s duration pulses synchronized by the laser pulses. The photomultiplier signals are integrated during the 100 to 300 ns time gates, which are adjusted to the time lapse of the returning fluorescence signal following a laser pulse emission, i.e., taking the sampling distance into account. Two measurements are performed during a laser pulse period. The first is done when the fluorescence signal is received and acquires both the fluorescence and the daylight background signal. The second measurement is done between laser pulses and acquires the background signal only, which is then subtracted from the fluorescence signal. These technical solutions enable us to detect oil fluorescence under bright daylight conditions without causing a nonlinear response of photomultipliers,

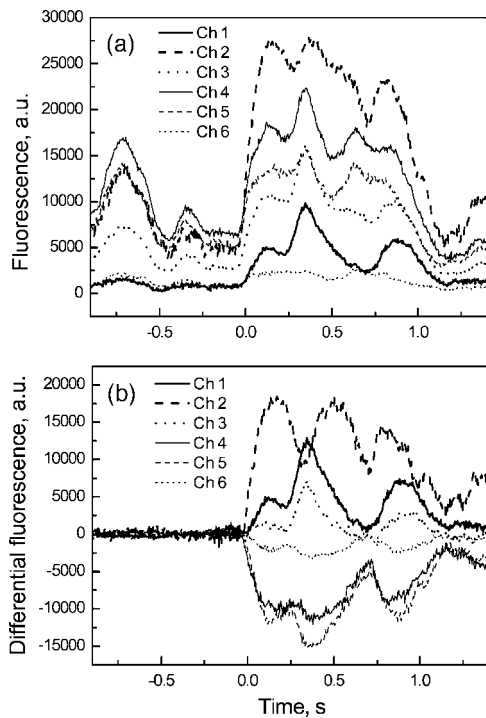


Fig. 4. (a) Time sequence of fluorescence signals measured on Lake Skaistis. The Arabian medium crude oil and the diethylether mixture were spilled at $t = 0$. (b) The same time sequence after data processing.

even in most cases when the sunlight is directly reflected from the water surface to the detection system. If the photomultiplier tube saturation still occurs, these data are recognized by the data acquisition program and are deleted. For shipboard applications the fluorosensor is equipped with a position-stabilized platform, which maintains the horizontal scanner position when the boat swings.

4. Results

For a demonstration of the fluorosensor operation, we present the field measurements obtained in Lithuania on the coast of Lake Skaistis near Vilnius and on a beach of the Baltic Sea. On Lake Skaistis the fluorosensor was situated 3 m above the water surface, and the laser beam was directed to the water surface over a 35 m distance. The wind caused 5–10 cm high waves. To obtain a thin and homogeneous oil film the oil samples were dissolved in diethylether at a concentration of 1:10. A volume of 3 ml of the solution was spilled on the water surface at the laser beam position. The solution rapidly spread to an area of 100–200 cm² and after the ether evaporated, an oil film of a few micrometers thickness was obtained. The films remained stable for several seconds, which was sufficient to measure their fluorescence. Later, the films spread to an area of approximately 1 m², forming a submicrometer film.

As an example of the measurement results Fig. 4 shows the time sequences of the fluorescence signals obtained before and after spilling the motor lubricant

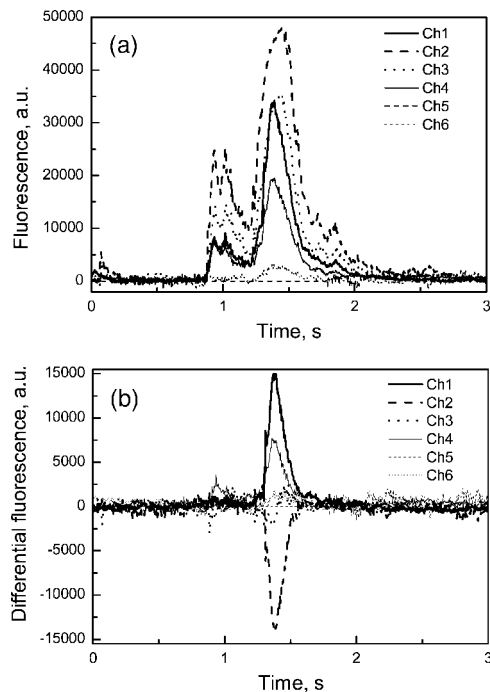


Fig. 5. (a) Time sequence of the fluorescence signals measured at the Baltic Sea. At approximately 1.25 s time, the laser beam targeted the motor lubricant spot. (b) The same time sequence after data processing.

and the diethylether mixture. Before the oil spill the water shows a clearly observable fluorescence of dissolved and dispersed organic matter. The fluorescence intensity fluctuated because of the waves. At the moment when the oil sample was spilled, the fluorescence signals increased, but this was masked by a signal variability caused by waves. Similar results were obtained with other samples. It should also be mentioned that the channel sensitivities were not spectrally calibrated. Relatively large spectral windows made the calibration problematic and not very useful. For these reasons, one cannot make a definite decision about the presence of oil fluorescence from the raw data.

Figure 5 shows similar data obtained on a beach of the Baltic Sea. The fluorosensor was situated approximately 2 m above sea level and directed at waves from a distance of approximately 40 m. Then 100 ml of motor lubricant was spilled into the rolling sea. In this case, the fluorescence was observed only at some particular wave positions, when the laser beam was directed to the front edge of the wave. The information about the presence of the oil pollution was completely hidden by the signal variability.

5. Discussion

The possibility of identifying and classifying oils and their products from their laser-induced fluorescence spectra is widely discussed in the literature. Broad and structureless emission spectra, modifications of the spectra due to oil weathering and the presence of natural water fluorescence make this task rather difficult

to perform.⁶ Patsayeva *et al.*¹⁰ argue that emission spectra alone do not constitute a decisive fingerprinting criterion for oil identification. They suggest supporting fluorescence data with fluorescence lifetime and water Raman signal suppression data. Alaruri *et al.*¹¹ demonstrated that a combination of fluorescence spectra under four different excitation wavelengths and fluorescence lifetime data is sufficient to classify oils into several categories. On the other hand, Dolenko *et al.*¹² argued that data analysis based on an artificial neural network (ANN) approach enables us to separate oil fluorescence from natural water fluorescence even when the latter is much stronger. Their approach is based on the similarity of the fluorescence spectra of unpolluted water taken from different Black Sea positions.

The Baltic Sea water fluorescence differs from that of the Black Sea. However, despite a more than three times difference in intensity, the shapes of the spectra of samples taken from different Baltic Sea locations are almost identical (see Fig. 6). The spectrum of the Lake Skaistis water is also quite similar. The different relative intensity of the Raman scattered light in these spectra is a result of their normalization to the fluorescence band maximum. The Raman signal is relatively weak because of the strong fluorescence of coastal water samples. Identical background spectra enable detection of small fluorescence spectra variations related to the oil pollution. However, because of the wave-induced signal variability the water fluorescence background cannot be simply subtracted and, as was demonstrated, the oil pollution cannot be determined from the raw fluorescence data.

To visualize the fluorescence changes we used the data processing method resembling the ANN approach. The signals of the different channels obtained from the unpolluted water were normalized to the sum of all the channel signals, yielding relative signal intensities of the natural water fluorescence. The same procedure was applied to the signals taken after the oil spill. The relative intensities of natural water fluorescence were then subtracted from those obtained from the oil-polluted water. Finally, the obtained result was multiplied by the sum of all the channel signals. The last procedure was necessary to take into account the different oil detection accuracies obtained from different fluorescence signals; i.e., differential signals were enhanced at time intervals when the fluorescence was strong and were suppressed at time intervals when the fluorescence was weak. Equation (3) describes the calculation procedure:

$$\begin{aligned} \text{Ch}_i^{\text{dif}} &= \left[\frac{\text{Ch}_i^{\text{oil}}}{\sum_n \text{Ch}_n^{\text{oil}}} - \left(\frac{\text{Ch}_i^{\text{water}}}{\sum_n \text{Ch}_n^{\text{water}}} \right) \right] \sum_n \text{Ch}_n^{\text{oil}} \\ &= \text{Ch}_i^{\text{oil}} - \sum_n \text{Ch}_n^{\text{oil}} \left(\frac{\text{Ch}_i^{\text{water}}}{\sum_n \text{Ch}_n^{\text{water}}} \right). \end{aligned} \quad (3)$$

Here Ch_i^{dif} is the difference signal of channel i calcu-

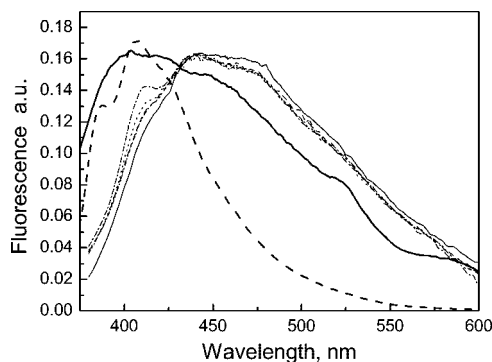


Fig. 6. Comparison of fluorescence spectra of Arabian medium crude oil (thick solid curve), motor lubricant (dashed thick curve), and natural water fluorescence spectra of samples taken from different Baltic Sea and Curonian Lagoon sites (thin dashed and dotted curves) and from Lake Skaistis (thin solid curve). The spectra were measured with a PerkinElmer LS 50B fluorimeter at a 355 nm excitation wavelength. The spectra are corrected for the apparatus function.

lated from the channel i signal values measured in the presence of oil film (Ch_i^{oil}) and in its absence ($\text{Ch}_i^{\text{water}}$). Figures 4(b) and 5(b) present the transformed data. Positive and negative normalized signal values express differences between the oil and the natural water fluorescence spectra. For the Lake Skaistis measurements [Fig. 4(b)] the fluorescence intensity increases in the first three channels and decreases in last three channels in agreement with the stationary fluorescence spectra. In the Baltic Sea the signal in channel 2 decreases. This is evidently because undiluted motor lubricant was spilled in this case, which completely absorbed excitation light and eliminated the Raman scattered light, which normally contributes to the signal in channel 2. The fluctuating water fluorescence is effectively eliminated by this data transformation procedure even in the case of laser targeting into breaking waves. Non-zero difference signal values appear only in the presence of oil fluorescence.

The normalized differential fluorescence signals clearly indicate the presence of an anomalous fluorescence signature, i.e., water pollution. However, the pollutant fluorescence spectra cannot be reconstructed from the normalized fluorescence data because the information about the original distribution of the pollutant and the natural water fluorescence intensities is lost due to the normalization. Such reconstruction is possible from raw fluorescence data only when pollutant fluorescence strongly dominates over the natural water fluorescence background. In the case of coastal waters such a situation may probably appear only if the water is completely covered by the nontransparent oil layer. However, even in this case additional information about the presence of a thick oil film is necessary because the fluorescence spectra give no such criterion.

Raman scattering in the water column may be used as a criterion of the oil film thickness estimation.^{13,14} The Raman signal has also been shown to be useful

for oil film detection¹⁵ and for fluorescence data normalization.¹² In coastal areas, the Raman signal becomes less informative. The water turbidity reduces the excitation light penetration depth and the water Raman signal. Moreover, changes in turbidity may cause variation in the Raman signal intensity. Nevertheless, the absence of the Raman signal in the presence of strong fluorescence may serve as an indication of optically thick oil films.

6. Concluding Remarks

We have analyzed the technical problems related to the fluorescence lidar application onboard ship or onshore for oil spill detection. The results of our investigation showed that reliable oil spill detection is possible at distances of up to approximately 50 m from several meters in height by day and by night by using a diode pumped solid-state laser with a relatively low pulse energy (approximately 1 mJ) and a 21 cm diameter fluorescence collecting telescope. The scanning distance significantly depends on the height of the instrument above the water surface and may be increased to approximately 100 m if the fluorosensor is situated at 10 m or higher. Waves, which are usually present on natural water surfaces, allow the scanning distance to be increased even more since the angular factor concerning the laser beam and the fluorescence reflection saturates when the scanning angle approaches the wavefront inclination angle. On the other hand, the waves cause a variability in the fluorescence signal and make discrimination between the oil and the water fluorescence more difficult. We have developed an approach that permits an efficient elimination of the natural water fluorescence. However, a reconstruction of the fluorescence spectrum of the pollutant and its identification is possible only when the pollutant fluorescence is much stronger than the natural water fluorescence. On the other hand, the identification of the pollutant is less important for an onshore or ship-based device because of the prospective operation specifics when the possible pollution sources are usually known.

The authors acknowledge the support of the Fifth Framework Programme of the European Community, contract EVK3-CT-2002-30001, for this work.

References

1. A. E. Lodge, ed., *Remote Sensing of Oil Slicks* (Wiley, 1989).
2. R. H. Goodman, *Simple Remote Sensing System for the Detec-*

- tion of Oil on Water*, Report 98 (Environmental Studies Research Fund, 1997), p. 31.
3. S. Bagheri, M. Stein, and C. Zetlin, "Utility of airborne videography as an oil spill-response monitoring system," in *Encyclopedia of Environmental Control Technology* (Gulf Publishing, 1995), pp. 367–376.
4. M. F. Fingas, C. E. Brown, and J. V. Mullin, "The visibility limits of oil on water and remote sensing thickness detection limits," in *Proceedings of the Fifth Thematic Conference on Remote Sensing for Marine and Coastal Environments* (Environmental Research Institute of Michigan, 1998), pp. 411–418.
5. R. Dick, M. Fruhwirth, and C. Brown, "Laser fluorosensor work in Canada," in *Proceedings of the First Thematic Conference on Remote Sensing for Marine and Coastal Environments* (Environmental Research Institute of Michigan, 1992), pp. 223–236.
6. T. Hengstermann and R. Reuter "Laser remote sensing of pollution of the sea: a quantitative approach," European Association of Remote Sensing Laboratories, *Advances in Remote Sensing* 1 (1992), pp. 52–60.
7. R. Reuter, H. Wang, R. Willkomm, K. D. Loquay, T. Hengstermann, and A. Braun, "A laser fluorosensor for maritime surveillance: measurement of oil spills," European Association of Remote Sensing Laboratories *Advances in Remote Sensing* 3 (1995), pp. 152–169.
8. S. Babichenko, A. Dudelzak, J. Lapimaa, A. Lisin, L. Poryvkina, and A. Vorobiev, "Locating water pollution and shore discharges in coastal zone and inland waters with FLS lidar," European Association of Remote Sensing Laboratories *Proceedings* 5(1), 32–41 (2006).
9. S. A. Burikov, D. V. Klimov, P. N. Litvinov, D. V. Maslov, and V. V. Fadeev, "Shore-based lidar for monitoring coastal sea water areas," *Quantum Electron.* **31**, 745–750, (2001).
10. S. Patsayeva, V. Yuzhakov, V. Varlamov, R. Barbini, R. Fantoni, C. Frassanito, and A. Palucci, "Laser spectroscopy of mineral oils on the water surface," in *Proceedings of the European Association of Remote Sensing Laboratories, SIG Workshop Lidar*, Dresden, Germany (2000), pp. 106–114.
11. S. D. Alaruri, M. Rasas, O. A. S. Jubian, F. Al-Bahrani, and M. Quinn, "Remote characterization of crude and refined oils using a laser fluorosensor system," *Opt. Eng.* **34**, 214–221 (1995).
12. T. A. Dolenko, V. V. Fadeev, I. V. Gerdova, S. A. Dolenko, and R. Reuter, "Fluorescence diagnostics of oil pollution in coastal marine waters by use of artificial neuron networks," *Appl. Opt.* **41**, 5155–5166 (2002).
13. F. E. Hoge and R. N. Swift, "Oil film thickness measurement using airborne laser-induced water Raman backscatter," *Appl. Opt.* **19**, 3269–3281 (1980).
14. J. Piskozub, V. Drozdowska, and V. Varlamov, "A lidar system for remote measurement of oil film thickness on sea surface," in *Proceedings of the Fourth Thematic Conference on Remote Sensing for Marine and Coastal Environments* (Environmental Research Institute of Michigan, 1997), pp. 386–391.
15. T. Hengstermann and R. Reuter, "Lidar fluorosensing of mineral oil spills on the sea surface," *Appl. Opt.* **29**, 3218–3227 (1990).